DOI: 10.61782/fa.2025.0258

FORUM ACUSTICUM
EURONOISE 2025

CYLINDRICAL HARMONIC DECOMPOSITION OF THE SOUND INTENSITY VECTORS

Jiarui Wang* **Thushara Abhayapala**

The Australian National University, Canberra, Australia

ABSTRACT

Sound intensity is related to human's perception of sound at mid to high frequencies. Traditionally, sound intensity vector is measured at a sweet spot using an intensity probe. To cover a spatial region, the intensity probe must be placed at multiple sampling points. To reduce hardware cost and measurement complexity, this paper proposes the cylindrical harmonic coefficients of the sound intensity vectors (CH-I coefficients) in a circular listening area. The CH-I coefficients are derived from cylindrical microphone array measurements of the pressure in the circular listening area. Hence, there is no need to employ multiple intensity probes or move the intensity probe to different sampling points. For application, this paper proposes the intensity matching algorithm, which reproduces the sound intensity vectors in the circular listening area by matching the desired CH-I coefficients. Simulations show the proposed intensity matching algorithm accurately reproduces the sound intensity vectors and requires fewer loudspeakers than pressure-based method to achieve similar accuracy in reproduced sound intensity vectors.

Keywords: *Sound intensity vectors, cylindrical harmonics, spatial sound field reproduction.*

1. INTRODUCTION

In spatial sound field reproduction system, the aim is to reproduce the desired spatial perception to the listener. In many cases, spatial sound field reproduction concerns accurately reproducing the pressure throughout the listening region. Relevant methods include wave field synthesis [1–7] and higher-order Ambisonics [8–10]. Numerous loudspeakers are usually required, yet a high accuracy in the reproduced pressure alone does not translate to improved perception [11].

To improve perception, vector quantities such as the acoustic velocity vectors (AVVs), the energy vector and the sound intensity vectors were introduced to spatial sound field reproduction systems. The AVV is related to the Gerzon's velocity vector (a.k.a. the r_V vector), which is relevant to human's localisation of sound at low frequencies [12, 13]. The AVVs have been used in spatial sound field reproduction systems [14–21]. The spherical harmonic and the cylindrical harmonic decompositions of the AVVs have also been derived [16, 20–22]. The energy vector is also known as the Gerzon's energy vector or the r_E vector [12, 13]. The energy vector is widely used in Ambisonic decoding [14, 15].

This paper focuses on the sound intensity vectors, which are related to human's localisation of sound at mid to high frequencies [23]. Sound intensity vectors can be matched at multiple sampling points within the listening region [24] or can be used to control the planarity of the reproduced sound field [25]. The spherical harmonic decomposition of the sound intensity vectors were introduced in [23] and were used in reproduction at multiple sweet spots [26] and in multiple listening zones [27], This paper reduces the listening region to a two-dimensional (2D) circular area, which can be on the plane where listener's ears are located. 2D scenarios are useful when installing a spherical loudspeaker array is impractical. A 2D sound field is often described using cylindrical harmonic expansion. This paper derives the cylindrical harmonic coefficients of the sound intensity vectors (CH-I). To use

**Corresponding author*: u5879960@anu.edu.au.

Copyright: *©2025 Jiarui Wang et al. This is an open-access article distributed under the terms of the Creative Commons Attribution 3.0 Unported License, which permits unrestricted use, distribution, and reproduction in any medium, provided the original author and source are credited.*

CH-I coefficients in spatial sound field reproduction system, this paper proposes intensity matching (IM), which matches the CH-I coefficients on the boundary of the listening area. Simulation shows that when compared with pressure matching, IM results in a higher accuracy in the reproduced sound intensity vectors throughout the listening area.

2. SOUND INTENSITY VECTORS IN A LISTENING AREA

This paper concerns the sound field in a circular listening area. In polar coordinate system, a point $\mathbf{r} = (r, \phi)$ in which the radius $r = ||\mathbf{r}||$ and the azimuth angle ϕ is defined counterclockwise from the positive x-axis. The pressure in a circular listening area can be measured by a cylindrical microphone array. The cylindrical harmonic decomposition of the pressure is of the form

$$p(k, r, \phi) = \sum_{n=-N}^{N} \alpha_n(k) J_n(kr) e^{in\phi} \tag{1}$$

in which k is the wavenumber, $\alpha_n(k)$ represents the cylindrical harmonic coefficients of the pressure, $J_n(\cdot)$ denotes Bessel function of the first kind and N is the truncation order. It was shown in [21] that by using the sound field translation formula, the AVVs in the listening area can also be expressed using cylindrical harmonic decomposition of the form

$$v_{\hat{\boldsymbol{e}}}(k, r, \phi) = \sum_{m=-N+1}^{N-1} (\beta_{\hat{\boldsymbol{e}}})_m(k) J_m(kr) e^{im\phi} \tag{2}$$

in which $\hat{\boldsymbol{e}} \in \{\hat{\boldsymbol{x}}, \hat{\boldsymbol{y}}\}$ and $(\beta_{\hat{\boldsymbol{e}}})_m(k)$ denotes the cylindrical harmonic coefficients of the AVVs. $(\beta_{\hat{\boldsymbol{e}}})_m(k)$ is related to $\alpha_n(k)$ via

$$(\beta_{\hat{\boldsymbol{x}}})_m(k) = \frac{1}{2} \frac{i}{\rho_0 c} [\alpha_{m+1}(k) - \alpha_{m-1}(k)] \tag{3}$$

$$(\beta_{\hat{\boldsymbol{y}}})_m(k) = -\frac{1}{2} \frac{1}{\rho_0 c} [\alpha_{m+1}(k) + \alpha_{m-1}(k)] \tag{4}$$

in which c is the speed of sound and ρ_0 is the density of air. The derivation of (3) and (4) is covered in [21].

The sound intensity vector is defined as

$$I_{\hat{\boldsymbol{e}}}(k, r, \phi) = p(k, r, \phi)\, \overline{v_{\hat{\boldsymbol{e}}}(k, r, \phi)} \tag{5}$$

in which $\overline{(\cdot)}$ denotes conjugation. Substituting (1) and (2) into (5) gives

$$\begin{aligned} I_{\hat{\boldsymbol{e}}}(k, r, \phi) =& \left(\sum_{n=-N}^{N} \alpha_n(k) J_n(kr) e^{in\phi} \right) \\ & \left(\sum_{m=-M}^{M} \overline{(\beta_{\hat{\boldsymbol{e}}})_m(k)} J_m(kr) e^{-im\phi} \right) \\ =& \sum_{n=-N}^{N} \sum_{m=-M}^{M} \alpha_n(k) \overline{(\beta_{\hat{\boldsymbol{e}}})_m(k)} J_n(kr) \\ & J_m(kr) e^{i(n-m)\phi} \end{aligned} \tag{6}$$

in which $M = N - 1$. The sound intensity vector can be expressed using cylindrical harmonic decomposition of the form

$$I_{\hat{\boldsymbol{e}}}(k, r, \phi) = \sum_{q=-Q}^{Q} (\gamma_{\hat{\boldsymbol{e}}})_q(k, r) e^{iq\phi} \tag{7}$$

in which the CH-I coefficients

$$\begin{aligned} (\gamma_{\hat{\boldsymbol{e}}})_q(k, r) =& \frac{1}{2\pi} \int_0^{2\pi} \sum_{n=-N}^{N} \sum_{m=-M}^{M} \alpha_n(k) \overline{(\beta_{\hat{\boldsymbol{e}}})_m(k)} J_n(kr) \\ & J_m(kr) e^{i(n-m)\phi} e^{-iq\phi} d\phi \\ =& \sum_{n=-N}^{N} \sum_{m=-M}^{M} \alpha_n(k) \overline{(\beta_{\hat{\boldsymbol{e}}})_m(k)} J_n(kr) J_m(kr) \\ & \frac{1}{2\pi} \int_0^{2\pi} e^{i(n-m-q)\phi} d\phi \\ =& \sum_{m=-M}^{M} \alpha_{m+q}(k) \overline{(\beta_{\hat{\boldsymbol{e}}})_m(k)} J_{m+q}(kr) J_m(kr). \end{aligned} \tag{8}$$

Equation (8) shows that the CH-I coefficients $(\gamma_{\hat{\boldsymbol{e}}})_q(k, r)$ are directly related to the cylindrical harmonic coefficients of the pressure $\alpha_n(k)$. Instead of placing an intensity probe at multiple sampling points in the listening area, the sound intensity vectors in the listening area can be calculated by manipulating $\alpha_n(k)$, which can be measured using a cylindrical microphone array. The CH-I coefficients can be truncated up to $Q = N + M$.

3. AVERAGE SOUND INTENSITY VECTOR IN A LISTENING AREA

The CH-I coefficients in (8) depend on the radial distance r. To cover the whole listening area, the CH-I coefficients

must be calculated on multiple concentric circles. When the listening area is small, it may be sufficient to calculate the average sound intensity vector in the listening area. The average sound intensity vector in a spherical listening region is covered in [22]. This paper focuses on the 2D case. Let R denote the radius of the listening area, the average sound intensity vector is defined as

$$\mathcal{I}_{\hat{\boldsymbol{e}}}(k) = \int_0^{2\pi}\int_0^R \zeta(k,r,\phi) I_{\hat{\boldsymbol{e}}}(k,r,\phi) r dr d\phi \quad (9)$$

in which $\zeta(k,r,\phi)$ is a real-valued weight function with cylindrical harmonic decomposition

$$\begin{aligned}\zeta(k,r,\phi) &= \sum_{b=-B}^{B} \xi_b(k,r) e^{ib\phi} \\ &= \sum_{b=-B}^{B} \overline{\xi_b(k,r)} e^{-ib\phi}. \end{aligned} \quad (10)$$

Substituting (10) and (7) into (9) gives

$$\begin{aligned}\mathcal{I}_{\hat{\boldsymbol{e}}}(k) =& \int_0^{2\pi}\int_0^R \left(\sum_{b=-B}^{B} \overline{\xi_b(k,r)} e^{-ib\phi}\right) \\ & \left(\sum_{q=-Q}^{Q} (\gamma_{\hat{\boldsymbol{e}}})_q(k,r) e^{iq\phi}\right) r dr d\phi \\ =& \sum_{b=-B}^{B}\sum_{q=-Q}^{Q} \int_0^R \overline{\xi_b(k,r)} (\gamma_{\hat{\boldsymbol{e}}})_q(k,r) \\ & \int_0^{2\pi} e^{i(q-b)\phi} d\phi\, r dr \\ =& 2\pi \sum_{b=-B}^{B} \int_0^R \overline{\xi_b(k,r)} (\gamma_{\hat{\boldsymbol{e}}})_b(k,r) r dr. \end{aligned} \quad (11)$$

Like [22], this paper assumes the real-valued weight function is angular independent, i.e., $\zeta(k,r,\phi) \equiv \zeta(k,r) = \xi_0(k,r) = \overline{\xi_0(k,r)}$. Equation (11) becomes

$$\mathcal{I}_{\hat{\boldsymbol{e}}}(k) = 2\pi \int_0^R \zeta(k,r) (\gamma_{\hat{\boldsymbol{e}}})_0(k,r) r dr. \quad (12)$$

Substituting (8) into (12) gives

$$\begin{aligned}\mathcal{I}_{\hat{\boldsymbol{e}}}(k) =& 2\pi \int_0^R \zeta(k,r) \sum_{m=-M}^{M} \alpha_m(k) \overline{(\beta_{\hat{\boldsymbol{e}}})_m(k)} \\ & [J_m(kr)]^2 r dr \\ =& \sum_{m=-M}^{M} \alpha_m(k) \overline{(\beta_{\hat{\boldsymbol{e}}})_m(k)}\, \mathcal{G}_m(k) \end{aligned} \quad (13)$$

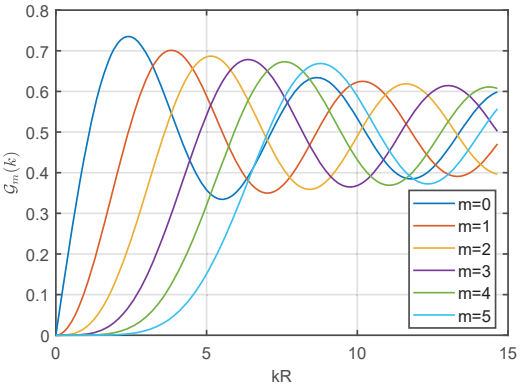

Figure 1. Amplitude of $\mathcal{G}_m(k)$ with upper summation limit $\mu = 50$.

in which

$$\mathcal{G}_m(k) = 2\pi \int_0^R \zeta(k,r) [J_m(kr)]^2 r dr. \quad (14)$$

As an example, suppose the weight function $\zeta(k,r) = k^2/(2\pi)$,

$$\begin{aligned}\mathcal{G}_m(k) &= \int_0^R k^2 [J_m(kr)]^2 r dr \\ &= \int_0^R (kr)[J_m(kr)]^2 k dr \\ &= \int_0^{kR} (kr)[J_m(kr)]^2 d(kr) \quad (15) \\ &= 2\sum_{\mu=0}^{\infty} (m+1+2\mu)[J_{m+1+2\mu}(kR)]^2 \quad (16) \end{aligned}$$

in which property 10.22.27 in [28] is used to convert the integral in (15) to the summation in (16). Figure 1 shows the amplitude of $\mathcal{G}_m(k)$. The amplitude converges to 0.5.

4. INTENSITY MATCHING

This section presents intensity matching (IM), which reproduces the desired sound field by matching the desired CH-I coefficients on the boundary of the listening area. In the recording stage, a cylindrical microphone array first captures the cylindrical harmonic coefficients $\alpha_n^{(\mathrm{d})}(k)$ of the desired pressure. Next, the cylindrical harmonic coefficients $(\beta_{\hat{\boldsymbol{e}}})_m^{(\mathrm{d})}(k)$ of the desired AVVs are calculated by using (3) and (4). Then, the desired CH-I coefficients $(\gamma_{\hat{\boldsymbol{e}}})_q^{(\mathrm{d})}(k,r)$ on the boundary of the listening area are found by using (8). A similar process is used to find the

CH-I coefficients $(\gamma_{\hat{\boldsymbol{e}}})_q^{(\ell)}(k,r)$ when the input to the ℓ-th loudspeaker with $\ell \in \{1,2,\cdots,L\}$ is a unit sinusoidal signal. In the reproduction stage, the squared weights of the loudspeakers are found by solving a system of equations

$$\boldsymbol{\gamma}^{(\mathrm{d})}(k,r) = \mathbf{H}(k,r)|\mathbf{w}(k)|^2. \tag{17}$$

Let $[\cdot]^T$ denote matrix transpose, the column vector

$$\begin{aligned}&\boldsymbol{\gamma}^{(\mathrm{d})}(k,r)\\ =&\big[\mathrm{Re}\{\boldsymbol{\gamma}_{\hat{\boldsymbol{x}}}^{(\mathrm{d})}(k,r)^T\},\mathrm{Im}\{\boldsymbol{\gamma}_{\hat{\boldsymbol{x}}}^{(\mathrm{d})}(k,r)^T\},\mathrm{Re}\{\boldsymbol{\gamma}_{\hat{\boldsymbol{y}}}^{(\mathrm{d})}(k,r)^T\},\\ &\mathrm{Im}\{\boldsymbol{\gamma}_{\hat{\boldsymbol{y}}}^{(\mathrm{d})}(k,r)^T\}\big]^T\end{aligned} \tag{18}$$

in which the column vector $\boldsymbol{\gamma}_{\hat{\boldsymbol{e}}}^{(\mathrm{d})}(k,r)$ is the concatenation of $(\gamma_{\hat{\boldsymbol{e}}})_q^{(\mathrm{d})}(k,r)$. The matrix

$$\mathbf{H}(k,r) = [\boldsymbol{\gamma}^{(1)}(k,r),\boldsymbol{\gamma}^{(2)}(k,r),\cdots,\boldsymbol{\gamma}^{(L)}(k,r)] \tag{19}$$

in which the ℓ-th column

$$\begin{aligned}&\boldsymbol{\gamma}^{(\ell)}(k,r)\\ =&\big[\mathrm{Re}\{\boldsymbol{\gamma}_{\hat{\boldsymbol{x}}}^{(\ell)}(k,r)^T\},\mathrm{Im}\{\boldsymbol{\gamma}_{\hat{\boldsymbol{x}}}^{(\ell)}(k,r)^T\},\mathrm{Re}\{\boldsymbol{\gamma}_{\hat{\boldsymbol{y}}}^{(\ell)}(k,r)^T\},\\ &\mathrm{Im}\{\boldsymbol{\gamma}_{\hat{\boldsymbol{y}}}^{(\ell)}(k,r)^T\}\big]^T\end{aligned} \tag{20}$$

with $\boldsymbol{\gamma}_{\hat{\boldsymbol{e}}}^{(\ell)}(k,r)$ being the concatenation of $(\gamma_{\hat{\boldsymbol{e}}})_q^{(\ell)}(k,r)$. The squared weights

$$|\mathbf{w}(k)|^2 = [|w^{(1)}(k)|^2,|w^{(2)}(k)|^2,\cdots,|w^{(L)}(k)|^2]^T. \tag{21}$$

in which $w^{(\ell)}(k)$ is the weight of the ℓ-th loudspeaker. Since the squared weights are non-negative, they can be solved by using the non-negative least squares method. The weights can then be found by first taking the square roots of the squared weights, followed by finding a suitable minimum-phase system through Hilbert transform.

This paper compares IM with the traditional pressure matching (PM) approach. In PM, the desired sound field is reproduced by matching the cylindrical harmonic coefficients of the desired pressure in the listening area. Similar to (17), the system of equations for PM is

$$\boldsymbol{\alpha}^{(\mathrm{d})}(k) = \mathbf{G}(k)\mathbf{w}(k). \tag{22}$$

The column vector $\boldsymbol{\alpha}^{(\mathrm{d})}(k)$ is the concatenation of $\alpha_n^{(\mathrm{d})}(k)$. The matrix

$$\mathbf{G}(k) = [\boldsymbol{\alpha}^{(1)}(k),\boldsymbol{\alpha}^{(2)}(k),\cdots,\boldsymbol{\alpha}^{(L)}(k)] \tag{23}$$

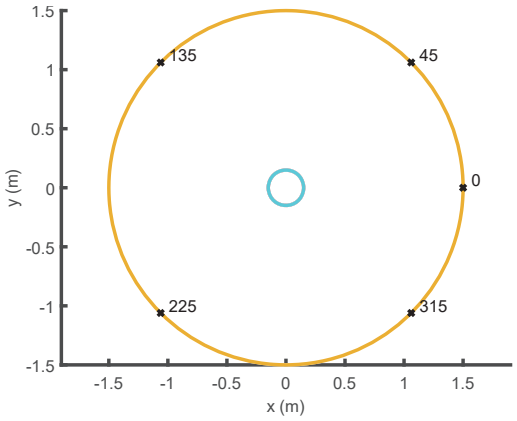

Figure 2. Simulation setup. The listening area is bounded by the cyan circle of radius 0.15 m. The loudspeakers denoted by "x" are located on the yellow circle of radius 1.5 m.

in which the ℓ-th column is the concatenation of $\alpha_n^{(\ell)}(k)$, which represents the cylindrical harmonic coefficients of the pressure when the input to the ℓ-th loudspeaker is a unit sinusoidal signal. The weights

$$\mathbf{w}(k) = [w^{(1)}(k),w^{(2)}(k),\cdots,w^{(L)}(k)]^T. \tag{24}$$

The weights can be solved by using Moore-Penrose pseudoinverse or Tikhonov regularisation.

Figure 2 shows the simulation setup. The circular listening area bounded by the cyan circle is 0.15 m in radius. The loudspeakers are located on a circle of 1.5 m radius. The azimuth angles of the loudspeakers are $[0,\pi/4,3\pi/4,5\pi/4,7\pi/4]$ rad. The loudspeakers are assumed to be infinite line sources with cylindrical harmonic coefficients

$$\alpha_n^{(\ell)}(k) = \frac{-i}{4}H_n^{(2)}(kr_\ell)e^{-in\phi_{(\ell)}} \tag{25}$$

in which $H_n^{(2)}(\cdot)$ is the Hankel function of the second kind. The desired sound field is a plane wave with incident direction $\phi_{\mathrm{pw}} = 8\pi/9$ rad. The cylindrical harmonic coefficients of the desired pressure are

$$\alpha_n^{(\mathrm{d})}(k) = i^n e^{-in\phi_{\mathrm{pw}}}. \tag{26}$$

The cylindrical harmonic coefficients of the pressure in (25) and (26) are truncated to ± 3. As a consequence, the CH-I coefficients are truncated to $q = \pm 5$. At each wavenumber k, the dimension of $\mathbf{H}(k)$ is 44-by-5 and the dimension of $\mathbf{G}(k)$ is 7-by-5. The squared weights in (17) are found by using the `lsqnonneg` function in

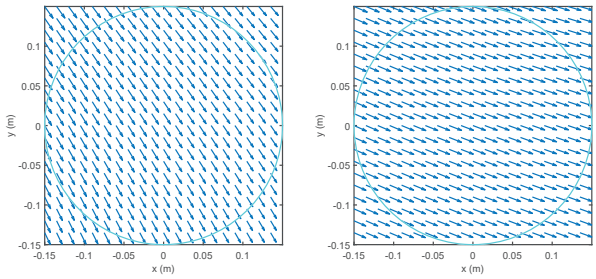

Figure 3. Real part of the reproduced sound intensity vectors at 800 Hz. The desired sound field is a plane wave with incident direction $8\pi/9$ rad. (a) is obtained from PM, whereas (b) is obtained from the proposed IM.

MATLAB and the weights in (22) are found by using the `pinv` function in MATLAB with the default tolerance.

Figure 3 illustrates the reproduced sound intensity vectors at 800 Hz. Figure 3(a) is from PM and Figure 3(b) is from the proposed IM. The reproduced sound intensity vectors from IM closely align with the direction of arrival of the desired plane wave, whereas the reproduced sound intensity vectors from PM deviate from the desired direction. The performance is evaluated as in [29] and [23]. The direction error

$$\epsilon(k) = \cos^{-1}(\mathrm{DOT}(k)) \text{ rad} \tag{27}$$

with

$$\mathrm{DOT}(k) = \frac{\mathbf{I}^{(\mathrm{d})}(k,\mathbf{r})}{||\mathbf{I}^{(\mathrm{d})}(k,\mathbf{r})||_2} \cdot \left[\frac{\mathbf{I}^{(\mathrm{r})}(k,\mathbf{r})}{||\mathbf{I}^{(\mathrm{r})}(k,\mathbf{r})||_2}\right]^T \tag{28}$$

in which the desired sound intensity vector $\mathbf{I}^{(\mathrm{d})}(k,\mathbf{r}) = [I^{(\mathrm{d})}_{\hat{\boldsymbol{x}}}(k,\mathbf{r}), I^{(\mathrm{d})}_{\hat{\boldsymbol{y}}}(k,\mathbf{r})]$ and the reproduced sound intensity vector $\mathbf{I}^{(\mathrm{r})}(k,\mathbf{r}) = [I^{(\mathrm{r})}_{\hat{\boldsymbol{x}}}(k,\mathbf{r}), I^{(\mathrm{r})}_{\hat{\boldsymbol{y}}}(k,\mathbf{r})]$. Figure 4 shows the average direction errors in the real part of the reproduced sound intensity vectors. The direction errors are averaged across 317 evaluation points within the cyan circle of radius 0.15 m in Figure 2. IM consistently achieves lower direction errors. Note that the direction error will change if the desired plane wave is from a different direction. Future work will evaluate the performance of IM when a listener is present in the listening area. Future work will also consider different loudspeaker layouts.

5. CONCLUSION

This paper proposed the CH-I coefficients, which were the cylindrical harmonic coefficients of the sound intensity vectors on the boundary of the circular listening area. The CH-I coefficients were only defined on the boundary since they were unique to the radius of the circle. The CH-I coefficients were used in intensity matching, which reproduced the desired sound intensity vectors on the listening area's boundary. Simulation showed that intensity matching resulted in higher accuracy in the directions of the sound intensity vectors in the listening area when compared with pressure matching. This paper also proposed a formulation of average sound intensity vectors. The proposed formulation was independent of the radius of circle on which CH-I coefficients were calculated.

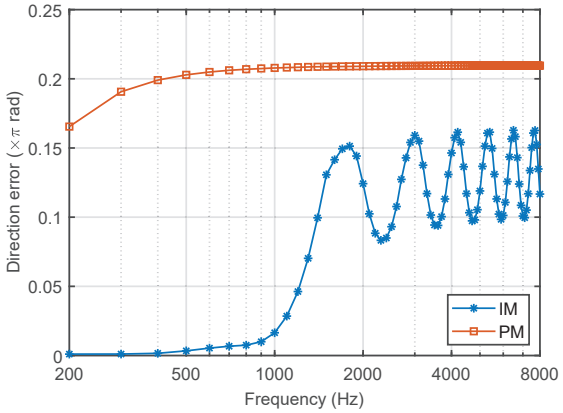

Figure 4. Direction errors in the reproduced sound intensity vectors.

6. REFERENCES

[1] A. J. Berkhout, D. de Vries, and P. Vogel, "Acoustic control by wave field synthesis," *The Journal of the Acoustical Society of America*, vol. 93, pp. 2764–2778, 05 1993.

[2] M. M. Boone, E. N. G. Verheijen, and P. F. van Tol, "Spatial sound-field reproduction by wave-field synthesis," *Journal of the Audio Engineering Society*, vol. 43, pp. 1003–1012, December 1995.

[3] J. Ahrens, R. Rabenstein, and S. Spors, "The theory of wave field synthesis revisited," *Journal of the Audio Engineering Society*, May 2008.

[4] P.-A. Gauthier and A. Berry, "Adaptive wave field synthesis for active sound field reproduction: Experimental results," *The Journal of the Acoustical Society of America*, vol. 123, pp. 1991–2002, 04 2008.

[5] F. Winter, F. Schultz, G. Firtha, and S. Spors, "A geometric model for prediction of spatial aliasing in 2.5 D sound field synthesis," *IEEE/ACM Transactions on Audio, Speech, and Language Processing*, vol. 27, no. 6, pp. 1031–1046, 2019.

[6] M. Buerger, R. Maas, H. W. Löllmann, and W. Kellermann, "Multizone sound field synthesis based on the joint optimization of the sound pressure and particle velocity vector on closed contours," in *2015 IEEE Workshop on Applications of Signal Processing to Audio and Acoustics (WASPAA)*, pp. 1–5, 2015.

[7] M. Buerger, C. Hofmann, and W. Kellermann, "Broadband multizone sound rendering by jointly optimizing the sound pressure and particle velocity," *The Journal of the Acoustical Society of America*, vol. 143, pp. 1477–1490, 03 2018.

[8] D. Ward and T. Abhayapala, "Reproduction of a plane-wave sound field using an array of loudspeakers," *IEEE Transactions on Speech and Audio Processing*, vol. 9, no. 6, pp. 697–707, 2001.

[9] T. Betlehem and T. D. Abhayapala, "Theory and design of sound field reproduction in reverberant rooms," *The Journal of the Acoustical Society of America*, vol. 117, pp. 2100–2111, 04 2005.

[10] M. A. Poletti, "Three-dimensional surround sound systems based on spherical harmonics," *Journal of the Audio Engineering Society*, vol. 53, pp. 1004–1025, November 2005.

[11] S. Spors, H. Wierstorf, A. Raake, F. Melchior, M. Frank, and F. Zotter, "Spatial sound with loudspeakers and its perception: A review of the current state," *Proceedings of the IEEE*, vol. 101, no. 9, pp. 1920–1938, 2013.

[12] M. A. Gerzon and G. J. Barton, "Ambisonic decoders for HDTV," in *Audio Engineering Society Convention 92*, Mar 1992.

[13] M. A. Gerzon, "General metatheory of auditory localisation," in *Audio Engineering Society Convention 92*, Mar 1992.

[14] D. Arteaga, "An ambisonics decoder for irregular 3D loudspeaker arrays," in *The 134th AES Convention*, 01 2013.

[15] F. Zotter and M. Frank, *Ambisonics: A Practical 3D Audio Theory for Recording, Studio Production, Sound Reinforcement, and Virtual Reality*. Springer, 2019.

[16] H. Zuo, T. D. Abhayapala, and P. N. Samarasinghe, "Particle velocity assisted three dimensional sound field reproduction using a modal-domain approach," *IEEE/ACM Transactions on Audio, Speech, and Language Processing*, vol. 28, pp. 2119–2133, 2020.

[17] H. Zuo, L. I. Birnie, P. N. Samarasinghe, T. D. Abhayapala, and V. Tourbabin, "Particle-velocity-based mixed-source sound field translation for binaural reproduction," *Applied Sciences*, vol. 13, no. 11, 2023.

[18] X. Hu, J. Wang, W. Zhang, and L. Zhang, "Time-domain sound field reproduction with pressure and particle velocity jointly controlled," *Applied Sciences*, vol. 11, no. 22, 2021.

[19] Y. Zhao, W. Zhang, and J. Chen, "A subband approach to personal sound zone with joint optimization of sound pressure and particle velocity," in *2023 Asia Pacific Signal and Information Processing Association Annual Summit and Conference (APSIPA ASC)*, pp. 427–431, 2023.

[20] F. J. Wang, T. D. Abhayapala, J. A. Zhang, and P. N. Samarasinghe, "Reproducing the acoustic velocity vectors in a spherical listening region," *IEEE Signal Processing Letters*, vol. 31, pp. 2220–2224, 2024.

[21] F. J. Wang, J. A. Zhang, T. Abhayapala, and P. Samarasinghe, "Reproducing the acoustic velocity vectors in a circular listening area," in *2024 17th International Conference on Signal Processing and Communication System (ICSPCS)*, pp. 1–5, 2024.

[22] A. Herzog and E. A. P. Habets, "Generalized intensity vector and energy density in the spherical harmonic domain: Theory and applications," *The Journal of the Acoustical Society of America*, vol. 150, pp. 294–306, 07 2021.

[23] H. Zuo, P. N. Samarasinghe, and T. D. Abhayapala, "Intensity based spatial soundfield reproduction using an irregular loudspeaker array," *IEEE/ACM Transactions on Audio, Speech, and Language Processing*, vol. 28, pp. 1356–1369, 2020.

[24] J.-W. Choi and Y.-H. Kim, "Manipulation of sound intensity within a selected region using multiple sources," *The Journal of the Acoustical Society of America*, vol. 116, pp. 843–852, 08 2004.

[25] Y. Huang, S. Zhao, and J. Lu, "Acoustic contrast control with a sound intensity constraint for personal sound systems," *The Journal of the Acoustical Society of America*, vol. 155, pp. 879–890, 02 2024.

[26] H. Zuo, P. N. Samarasinghe, and T. D. Abhayapala, "Intensity based soundfield reproduction over multiple sweet spots using an irregular loudspeaker array," in *2020 28th European Signal Processing Conference (EUSIPCO)*, pp. 486–490, 2021.

[27] H. Zuo, T. D. Abhayapala, and P. N. Samarasinghe, "3D multizone soundfield reproduction in a reverberant environment using intensity matching method," in *ICASSP 2021 - 2021 IEEE International Conference on Acoustics, Speech and Signal Processing (ICASSP)*, pp. 416–420, 2021.

[28] Digital Library of Mathematical Functions, "Integrals - Bessel and Hankel Functions." Accessed on April 8, 2025.

[29] L. Birnie, T. Abhayapala, V. Tourbabin, and P. Samarasinghe, "Mixed source sound field translation for virtual binaural application with perceptual validation," *IEEE/ACM Transactions on Audio, Speech, and Language Processing*, vol. 29, pp. 1188–1203, 2021.